



**ARTICLE**

# Effect of Introducing Conductive Organic Carrier on Properties of Low-Temperature Conductive Silver Paste

Peng Chen\*, Wentao Shi, Jian Wan and Lu Huang

Nanjing Institute of Materials Science for Electric Light Sources, Nanjing, 210015, China

\*Corresponding Author: Peng Chen. Email: colin158@163.com

Received: 10 May 2022 Accepted: 02 June 2022

## ABSTRACT

The poly(epoxy-N-methylaniline) conductive organic carrier was used as the bonding phase of the low-temperature conductive silver paste. Then, this was mixed with different proportions of silver powder to prepare the low-temperature conductive silver paste. Afterwards, the effect of the conductive organic carrier on the properties of the low-temperature conductive silver paste was determined by IR, DMA and SEM. The results revealed that the prepared conductive paste has good conductivity, film-forming performance, printing performance, low-temperature curing performance, and anti-aging performance. When the mass percentage of the bonding phase/conductive phase was 40/60, the lowest volume resistivity of the conductive silver paste was  $4.9 \times 10^{-6} \Omega \cdot \text{cm}$ , and the conductivity was the best.

## KEYWORDS

Low temperature conductive silver paste; poly(epoxy-N-methylaniline); volume resistivity; conductivity

## 1 Introduction

Under the context of carbon peak and carbon neutralization, industrial structures face profound challenges in low-carbon transformation. In the field of electronics, environmental protection materials have become a research hotspot, in terms of replacing and improving the power conversion efficiency of devices. Conductive silver paste is a key functional material in manufacturing photovoltaic devices, chip packaging and connections, 5G communication base stations, flexible displays, and transparent electrodes [1–6]. It is a composite material with conductivity, thermal conductivity and mechanical properties after process conditions (such as heating, pressurization, UV irradiation, etc.). Due to its environmental protection characteristics, this has gradually replaced the traditional welding process.

Low-temperature conductive silver paste (with a curing temperature of less than 300°C) is mainly formed by mixing silver powder (as the conductive phase and resin), a solvent, and other functional additives (as the bonding phase). The conductive film prepared through the screen printing process can be widely used for film switches, keyboards and RF antennas. This key technology has promoted the rapid development of the electronics industry [7]. At present, integrated electronic technology has enabled the conductive silver paste to have excellent printability, water resistance, hardness, adhesion, bending resistance and weather resistance, as well as higher conductivity [8,9]. The printing technology is also changing with each passing day. Among these, inkjet printing technology has received increasing



attention and research [10]. The present study did not use inkjet printing technology to investigate the printing performance.

The research and development of the performance of low-temperature conductive silver paste products in China are presently under exploration, in the aspects of the surface activation of conductive phase particles and doping of the adhesive phase insulating resin [11,12]. In researches conducted on these two aspects, the performance improvement of the conductive silver paste remained unsatisfactory, because the insulation resin was not conductive, and the cured resin had to be coated on the surface of the conductive phase particles, blocking the transmission of electrons. Furthermore, even when the content of silver powder was unilaterally increased to improve the conductivity and exceeded 80%, the printability, conductivity and film-forming effect of the conductive silver paste remained unsatisfactory [13,14].

In the present study, a poly(epoxy-N-methylaniline) conductive organic carrier was used to replace traditional adhesives, such as epoxy resin and phenolic resin, and mixed with silver powder, according to different proportions, in order to prepare the low-temperature conductive silver paste samples. Then, the conductivity, film-forming performance, printing performance and weather resistance of the samples were determined.

## 2 Experimental Section

### 2.1 Experimental Raw Materials

Conductive phase: Silver powder (self-made, flake/spherical, average particle size: 600 nm, specific surface area: 0.35–0.75 m<sup>2</sup>/g, tap density: 5.5 ± 1.0 g/cm<sup>3</sup>).

Bonding phase: N-methylaniline, (NH<sub>4</sub>)<sub>2</sub>S<sub>2</sub>O<sub>8</sub>, hydrochloric acid, ammonia, good solvent (acetone, butanone, DMF, DMSO, pyridine, or N-methylpyrrolidone), epichlorohydrin, and anhydrous AlCl<sub>3</sub> (as the catalyst); aniline, macromolecular proton acid (dodecylbenzene sulfonic acid or dodecyl sulfonic acid), mixed solvent (isophorone, butyl carbitol acetate and butyl carbitol), and organic gel additives.

### 2.2 Preparation of the Conductive Organic Carrier

#### 2.2.1 Preparation of the Poly(epoxy-N-methylaniline) Conductive Resin

- (1) Preparation of the epoxy-N-methylaniline (PMA<sub>n</sub>-g-Eo) prepolymer: N-methylaniline was used as the monomer and persulfate was used as the oxidant to synthesize the PMA<sub>n</sub> precursor in the hydrochloric acid aqueous solution (Formula (1), Fig. 1). Then, these were treated with ammonia to obtain the intrinsic PMA<sub>n</sub> polymer powder. Next, the PMA<sub>n</sub> precursor was prepared at a polymerization degree of 100–200 by controlling the polymerization time. Then, the PMA<sub>n</sub> was dissolved in the corresponding solvent (DMF, DMSO, pyridine and N-methylpyrrolidone), anhydrous AlCl<sub>3</sub> was used as the catalyst, and a number of epoxy groups were coupled on the aromatic ring of the PAn (Formula (2), Fig. 1), in order to obtain the epoxy-N-methylaniline (PMA<sub>n</sub>-g-Eo) prepolymer solution. Afterwards, the AlCl<sub>3</sub> catalyst and other solvents were filtered and removed, PMA<sub>n</sub>-g-Eo prepolymers with a bad solvent were precipitated, the unreacted monomer was eluted, and the PMA<sub>n</sub>-g-Eo prepolymer with a purity of more than 95% was obtained.
- (2) Preparation of the polyaniline curing agent: The PAn precursor was synthesized in hydrochloric acid aqueous solution, with aniline as the monomer and persulfate as the oxidant (Formula (3), Fig. 2). Then, polyaniline with 3–5 degrees of polymerization was prepared by controlling the coupling reaction time, in order to achieve good solubility in acetone, DMF, DMSO, and other solvents.
- (3) Ion doping of PAn derivatives: Intrinsic PAn derivatives require ion doping to obtain conductivity. Hence, macromolecular proton acid (dodecyl benzene sulfonic acid and/or dodecyl sulfonic acid) was used as the dopant (Ca<sup>2+</sup>, Mg<sup>2+</sup>, Zn<sup>2+</sup>, etc.) to introduce carriers to obtain the conductive

polymer. This part included the cationic doping of the polybenzidine curing agent (Formula (4), Fig. 3) and PMAn-g-Eo prepolymer (Formula (5), Fig. 3).

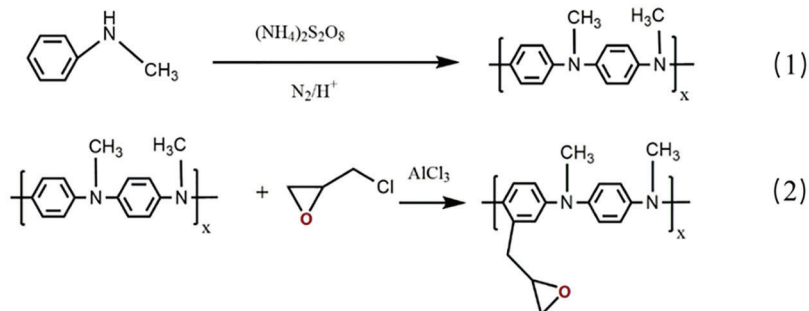


**Figure 1:** Synthesis of the epoxy-N-methylaniline prepolymer

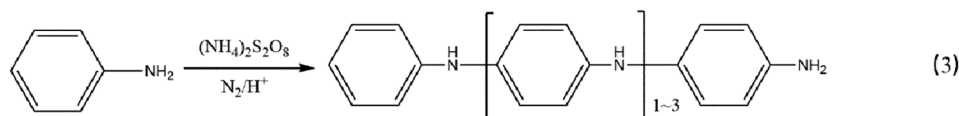


**Figure 2:** Synthesis of the polybenzidine curing agent

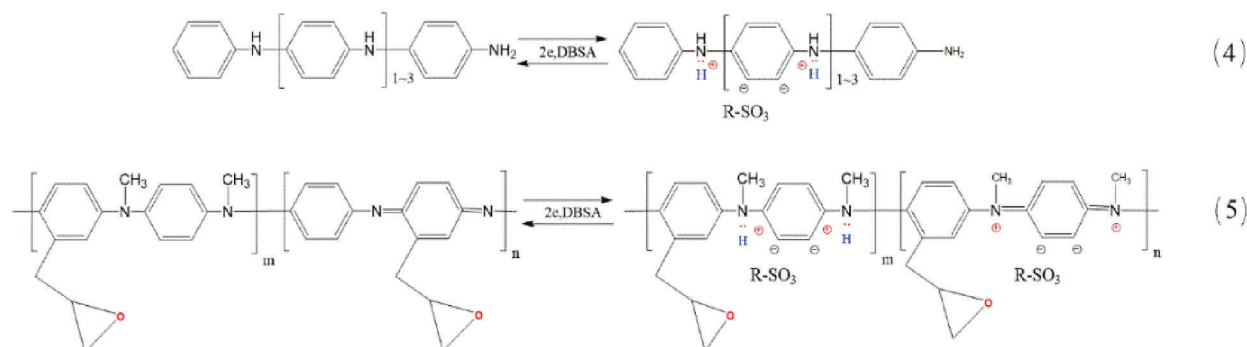


**Figure 3:** Schematic diagram for the ion doping of PAn derivatives

### 2.2.2 Preparation of the Conductive Organic Carrier

According to the mass ratio of each component listed in Table 1, the PMAn-g-Eo prepolymer, polyaniline curing agent, curing catalyst, viscosity reducing solvent and wetting agent, thixotropic agent, defoamer, antioxidant and other additives were mixed, and the conductive organic carrier was prepared after grinding, defoaming and defoaming.

**Table 1:** Mass percentage of each component of the conductive organic carrier

Component	Resin	Curing agent	Solvent	Auxiliary
Organic carrier	25%	3%	70%	2%

### 2.3 Preparation of the Low-Temperature Conductive Silver Paste

The conductive organic carrier of poly(epoxy-N-methylaniline) was mixed with the self-made silver powder in different proportions (Table 2). Then, these were grounded using a three-roller machine to obtain the conductive slurry samples with a fineness of  $<5 \mu\text{m}$ .

**Table 2:** Mass percentage of components of the low-temperature conductive silver paste

Sample	Conductive organic carrier	Self-made silver powder
Silver Paste-1	30%	70%
Silver Paste-2	35%	65%
Silver Paste-3	40%	60%
Silver Paste-4	45%	55%
Silver Paste-5	50%	50%

### 2.4 Testing and Characterization

Structural analysis of poly(epoxy-N-methylaniline): infrared (IR) spectrum; Thermal stability test (TG) of poly(epoxy-N-methylaniline): thermal weight loss; Dynamic thermomechanical analysis (DMA) of the low-temperature conductive silver paste: dynamic thermomechanical analyzer; Surface morphology analysis of the low-temperature conductive silver paste: scanning electron microscopy (SEM); Resistivity test of the low-temperature conductive silver paste: volume resistance meter; Bending resistance test after the low-temperature conductive silver paste was cured into the film: the cylindrical mandrel method ( $d = 1 \text{ mm}$ ) was used to confirm the crack and resistance change rate; Weather resistance test after the low-temperature conductive silver paste was solidified into the film: a weather resistance promotion tester was used, with a black panel temperature of  $85 \pm 1^\circ\text{C}$  and  $85 \pm 1\%$  humidity for 1,000 h, and it was determined whether discoloration and peeling occurred.

## 3 Results and Discussion

### 3.1 Performance Test of the Conductive Organic Carrier

#### 3.1.1 Conductivity Test

The poly(epoxy-N-methylaniline) adhesive resin for the poly(epoxy-N-methylaniline) conductive organic carrier was prepared from the N-methylaniline polymer and epichlorohydrin, and N-methylaniline was substituted with the epoxy groups by epichlorohydrin to enhance the welding tension of the low-temperature silver paste and adhesion of the substrate. In order to analyze the structural properties of N-methylaniline, before the substitution reaction, the intrinsic N-methylaniline polymer was tested by IR (Fig. 4).

Some studies have revealed that electrolyte composition has an impact on linear or cross-linked structures, and that there is a specific interaction between anions and bipolar ions. Compared with sulfate ions, bipolar ions are better shielded by perchlorate ions. In the whole polyaniline, the polaron lattice may be unevenly distributed. The electrochemical doping of polyaniline can lead to the balance between polaron and bipolar [15,16]. Its derivative N-methylaniline polymer is a conductive polymer with potential applications [17]. Compared with polyaniline, the pH sensitivity of N-methylaniline is not high, and the conductivity only depends on the oxidation state of the acidic medium [18,19]. N-methylaniline itself is a 1, 4-linked head tail structure, and this can be sub-divided into quinone and benzene structures. In Fig. 4,  $1,590 \text{ cm}^{-1}$  was the deformation vibration peak for the quinone structure, and  $1,500 \text{ cm}^{-1}$  was the deformation vibration peak for the benzene structure. The IR spectrum revealed that when the

concentration of  $(\text{NH}_4)_2\text{S}_2\text{O}_8$  was 0.2 M, the intensity of the deformation vibration peak of the benzene structure in eigenstate N-methylaniline was basically equivalent to that of the quinone structure. When the concentration of  $(\text{NH}_4)_2\text{S}_2\text{O}_8$  was increased, the IR spectrum revealed that the intensity of the deformation vibration peak of the quinone amino structure ( $1,590\text{ cm}^{-1}$ ) in the N-methylaniline polymer increased with the increase in oxidant concentration, when compared to the intensity of the deformation vibration peak of the benzene amino structure ( $1,590\text{ cm}^{-1}$ ). Therefore, increasing the oxidant concentration can increase the proportion of the quinone amino structure.

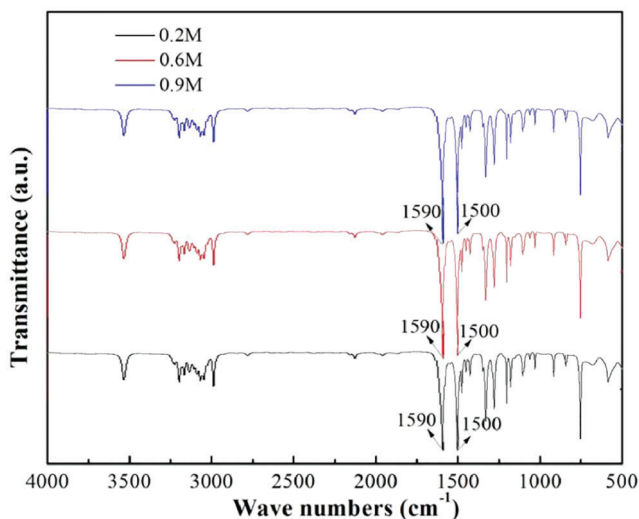


**Figure 4:** Infrared spectrum for the intrinsic N-methylaniline

The resistivity test revealed that the resistance of the N-methylaniline polymer initially decreased with the increase in  $(\text{NH}_4)_2\text{S}_2\text{O}_8$  oxidant concentration. When the oxidant concentration was greater than 0.9 M, the resistivity increased with the increase in its concentration. The changing trend is presented in Fig. 5.

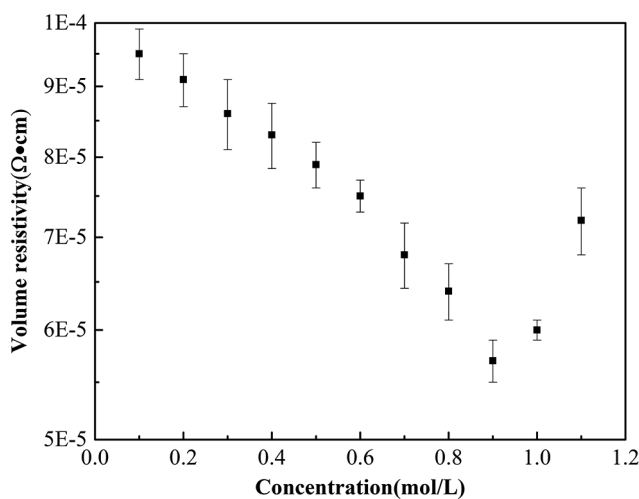


**Figure 5:** Volume resistivity curve

Considering that the low-temperature conductive silver paste was prepared by grinding and mixing the poly(epoxy-N-methylaniline) conductive organic carrier and silver powder using a three-roller machine, the silver powder was effectively dispersed in the poly(epoxy-N-methylaniline) conductive organic carrier, and the structural characteristics of the carrier did not change during the grinding process. Therefore, N-methylaniline polymers with a high proportion in the quinone amine structure exhibit better conductivity.

### 3.1.2 Thermal Stability Test

It has been reported that the redox stability of poly(N-methylaniline) is higher than that of its parent polymer polyaniline. Therefore, there is a need to test the thermal stability of this polymer [20,21]. Fig. 6 presents the thermogravimetric curve for intrinsic poly-N-methylaniline. It can be observed from the figure that as the temperature increased, the intrinsic poly-N-methylaniline polymer began to decompose at approximately 320°C, which was mainly caused by the thermal decomposition of small oligomer molecules in the polymer, indicating that intrinsic poly-N-methylaniline has good thermal stability. After reaching 380°C, the weight loss rate of the sample increased. Due to the weight loss caused by the decomposition reaction of the polyaniline main chain, the weight loss of the sample became nearly stable at 600°C. This shows that the molecular chain structure of intrinsic poly N-methylaniline is relatively stable, and has good heat resistance. Furthermore, the doped N-methylaniline polymer had certain environmental stability. The conductivity increased from  $1.0 \times 10^{-2}$  to  $8 \times 10^{-3}$  S/cm when this was placed indoors at 25°C for six months. Moreover, the thermal stability of poly(N-methylaniline) determines the thermal stability of the low-temperature conductive silver paste. After curing this into the film, the low-temperature conductive silver paste continued to maintain a good and stable contact under alternating temperature changes.

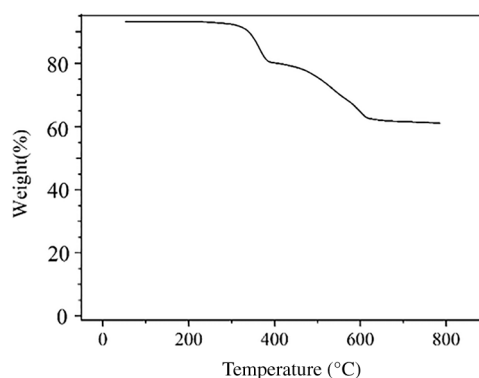


**Figure 6:** Thermogravimetric curve for intrinsic poly(N-methylaniline)

## 3.2 Performance Test for the Low-Temperature Conductive Silver Paste

### 3.2.1 Effect of the Carrier/Silver Powder Mass Ratio on the Performance of the Silver Paste

The prepared five silver paste samples were sintered at 180°C for one hour, and applied to the wafer with an area of  $8 \times 8 \text{ mil}^2$ , in order to make the device and test the conductivity. The results are presented in Fig. 7.

It can be observed from the figure that the volume resistance decreased with the increase in the content of the conductive organic carrier and the decrease in the content of the silver powder. When the mass percentage of the carrier/silver powder exceeded 40/60, the volume resistivity slowly increased. Furthermore, it was observed that the volume resistivity of the Silver Paste-3 sample was the best, which reached up to  $4.9 \times 10^{-6} \Omega \cdot \text{cm}$ . Compared to the volume resistivity of  $1.69 \times 10^{-4} \Omega \cdot \text{cm}$  of the Ag/AgCl conductive ink prepared by Thiago et al. [22] for screen printing electrodes, the volume resistivity of the Silver Paste-

3 sample was significantly lower than that of the Ag/AgCl conductive ink. Therefore, the conductivity of the Silver Paste-3 sample is better.

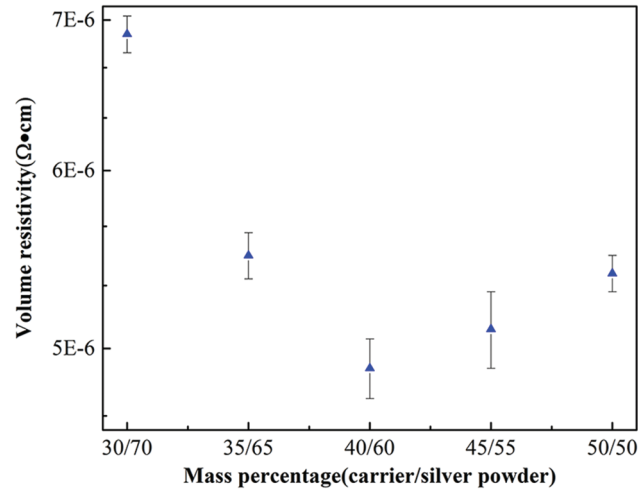


**Figure 7:** Volume resistivity curve

Although the conductive organic carrier has conductivity, the silver powder was used as the conductive phase for the conductive silver paste, and the minimum content threshold for the conductive organic carrier had the best effect of 60%.

### 3.2.2 Film Forming Performance Test of the Low-Temperature Silver Slurry

**Fig. 8** presents the SEM results for Silver Paste-3 after printing and leveling. It can be observed from the figure that the morphology of the sample was dense and flat.

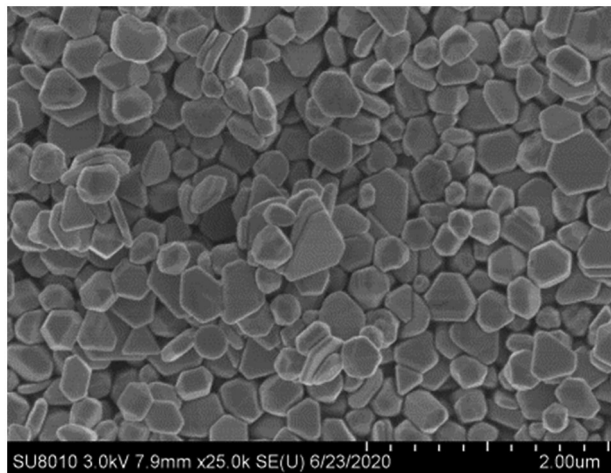


**Figure 8:** The SEM results after Silver Paste-3 printing and leveling

**Fig. 9** presents the SEM results for the grid line of Silver Paste-3 after low-temperature sintering at 180 °C/hour.

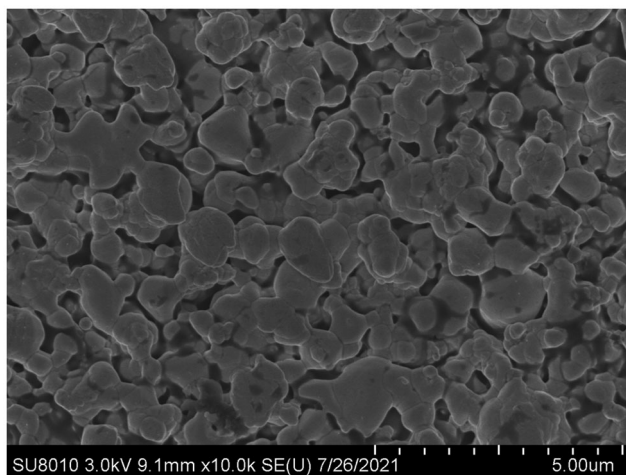


**Figure 9:** SEM results for the grid line after Silver Paste-3 sintering

Since the formation mechanism of the integral conductive network structure was that the poly(epoxy-N-methylaniline) bonding resin and polybenzidine curing agent contains the same aniline monomer, polybenzidine was cross-linked and cured with the epoxy group on the resin, and the end groups of the two polymers were coupled again to form the polyaniline of the system structure. Then, the introduced carriers formed a three-dimensional network conductive path, as shown in the SEM results. After sintering, the film formed a “molten” state, and the conductive organic carrier assisted the silver powder to form the conductive path of the film.

Adhesion is an important index for the silver paste. Ten wafer samples made of Silver Paste-3 were tested for solid crystal thrust (Fig. 10). As shown in the figure, under a stress area of  $8 \times 8 \text{ mil}^2$ , the thrust value of 10 samples was greater than twice that required by the enterprise standard.

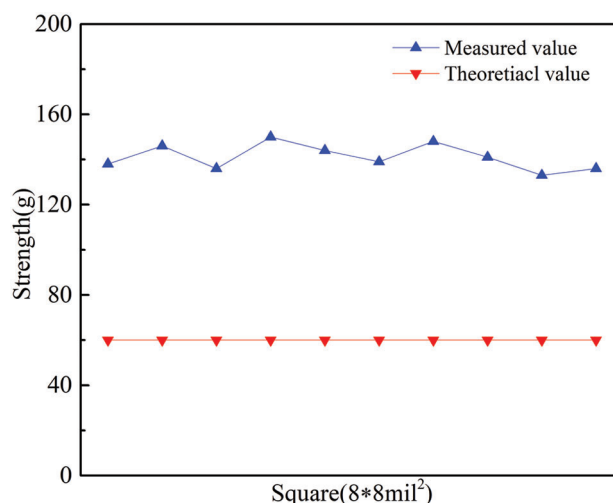


**Figure 10:** Test diagram for solid crystal thrust after Silver Paste-3 curing

Since the adhesion force comes from the conductive organic carrier of poly(epoxy-N-methylaniline), the conductive organic carrier enhanced the adhesion of the low-temperature silver paste, and improved the weather resistance of the film after curing.

These above results show that the conductive organic carrier of poly(epoxy-N-methylaniline) was cured at a low temperature. After the solvent was volatilized, the conductive organic carrier tightened the distance between silver powder particles, and improved the film-forming effect after sintering. Hence, the contradiction between the structural function and conductive function in the low-temperature conductive silver paste was solved, and high conductivity and strong bonding performance were realized.

### 3.2.3 Low-Temperature Silver Paste Printing Performance Test

Screen printing is a popular and simple method for printing metal interconnects on printed circuit boards. This coating technology can reduce costs, when compared to the cost of traditional vacuum deposition [23,24]. A 430/13-mesh screen was used in an ordinary printing machine to test the printing of the Silver Paste-3 samples. The printing line type, width and height, and printing effect are presented in Fig. 11 (screen opening: 30  $\mu\text{m}$ , printing speed: 250 mm/s, line width: 35  $\mu\text{m}$ ).

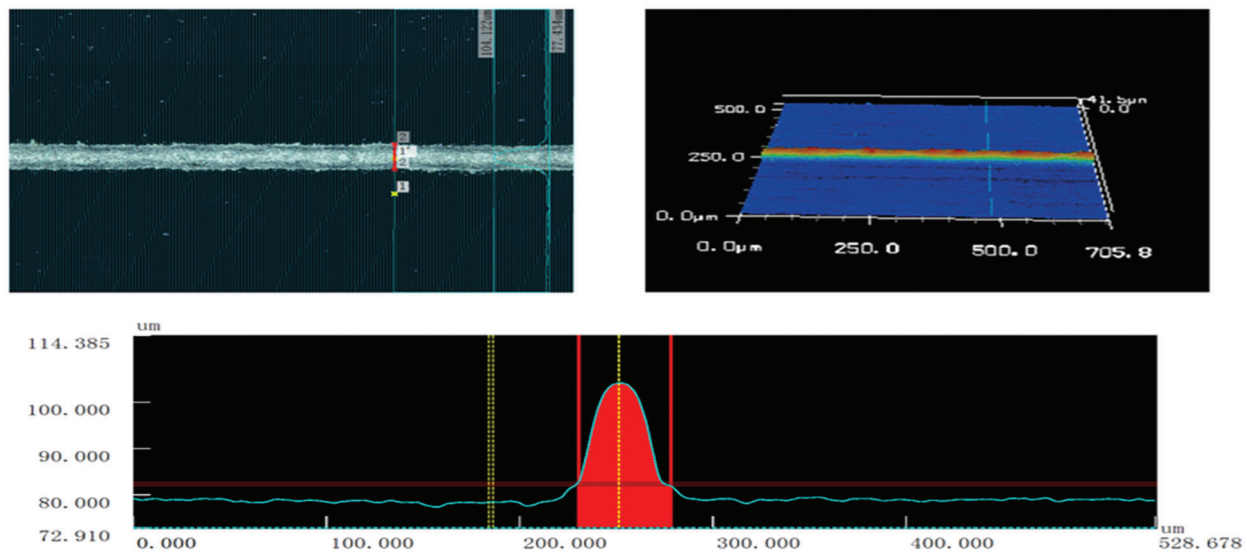


**Figure 11:** The 430/13-mesh screen printing effect on the fine grid line

The low-temperature curability of the low-temperature conductive silver paste was due to the conductive organic carrier of poly(epoxy-N-methylaniline). It can be observed that the epoxy groups on poly(epoxy-N-methylaniline) were bridged with each other through  $\text{Ca}^{2+}$ ,  $\text{Mg}^{2+}$  and  $\text{Zn}^{2+}$ . This solves the problem, in which the rigid molecular chains of polyaniline cannot be entangled, and exhibit a viscous flow. Furthermore, this realizes the long-term dimension of the film structure, and allows the low-temperature conductive silver paste to have good film-forming performance and printing performance.

### 3.2.4 Weather Resistance Test for the Low-Temperature Silver Paste

Fig. 12 presents the DMA curve for Silver Paste-3. In the figure, A, B and C represent the storage modulus, loss modulus, and loss factor curves, respectively. From the position and width of the peak in the C curve, it can be observed that the curing temperature for the low-temperature conductive silver paste was low, the glass transition temperature was 75°C, and the widening of glass transition temperature was conducive to the improvement in weather resistance of the composite [25–27].

Considering the instantaneous high temperature transfer of reflow soldering and wave soldering in the electronic packaging process [28–31], the solidified slurry film was required to have good bending resistance/toughness. The cylindrical mandrel method ( $d = 1 \text{ mm}$ ) was used for the silver paste in different mass ratios to confirm the crack and resistance change rate (Table 3).

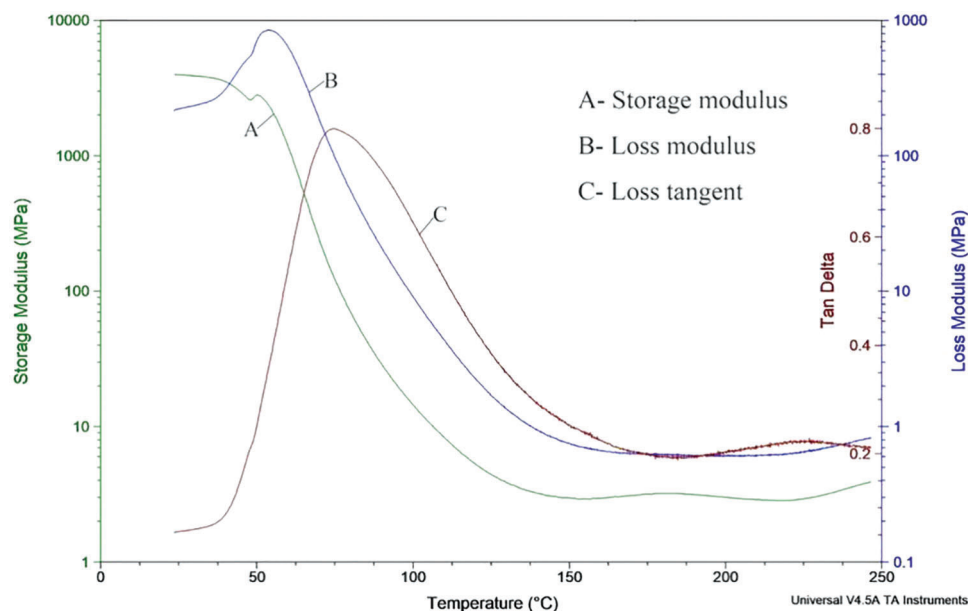


**Figure 12:** Glass transition temperature curve for Silver Paste-3

**Table 3:** Weather resistance test for the silver paste samples

Sample	Mass ratio	Volume resistivity ( $\Omega \cdot \text{cm}$ )	Bending resistance/ resistance change rate	Weather resistance
Silver Paste-1	30/70	$6.9 \times 10^{-6}$	No abnormality/ $\leq 10\%$	No discoloration or peeling
Silver Paste-2	35/65	$5.5 \times 10^{-6}$	No abnormality/ $\leq 10\%$	No discoloration or peeling
Silver Paste-3	40/60	$4.9 \times 10^{-6}$	No abnormality/ $\leq 10\%$	No discoloration or peeling
Silver Paste-4	45/55	$5.1 \times 10^{-6}$	No abnormality/ $\leq 10\%$	No discoloration or peeling
Silver Paste-5	50/50	$5.4 \times 10^{-6}$	No abnormality/ $\leq 10\%$	No discoloration or peeling

As shown in Table 3, the silver paste sample had good bending resistance and no abnormal fractures, and the resistance change rate of the film was  $\leq 10\%$ . The weather resistance of the five silver paste samples was tested using the weather resistance promotion tester. After 1,000 h of observation at a black panel temperature of  $85 \pm 1^\circ\text{C}$  with  $85 \pm 1\%$  humidity, the silver paste sample exhibited good weather resistance, without discoloration or peeling.

#### 4 Conclusion

- (1) For the conductive organic carrier synthesized in the present study, increasing the oxidant concentration ( $\leq 0.9 \text{ mol/L}$ ) can reduce the resistivity and improve the conductivity. The high conductivity slurry formed by the combination of the poly(epoxy-N-methylaniline) conductive organic carrier and silver powder had good conductivity, low temperature curing performance, and heat resistance. The conductive organic carrier is a new type of bonding phase material. Compared with traditional bonding resins, this has strong adhesion and high conductivity. The experimental results revealed that the volume resistivity of the conductive slurry decreased with the increase in the content of the conductive organic carrier and the decrease in silver powder content. However, the volume resistivity did not exhibit a decreasing trend when the silver

powder content was less than 60%. When the mass percentage of the bonding phase/conductive phase was 40/60, the volume resistivity of the high conductive slurry formed by the combination of the poly(epoxy-N-methylaniline) conductive organic carrier and silver powder was  $4.9 \times 10^{-6} \Omega\cdot\text{cm}$ . This was the conductive paste sample with the smallest volume resistivity and the best conductivity.

- (2) The conductive organic carrier of poly(epoxy-N-methylaniline) in the conductive slurry was prepared by mixing the poly(epoxy-N-methylaniline) bonding resin with the polyaniline curing agent, solvent and additives. The poly(epoxy-N-methylaniline) bonding resin and polyaniline curing agent contained the same aniline monomer. The polyaniline was crosslinked and cured with the epoxy group on the resin, the end groups of the two polymers could be coupled again to form the polyaniline of the system structure, and the introduced carriers formed a three-dimensional network conductive path to further assist the silver powder to form a conductive channel.
- (3) The good film-forming performance of the high conductivity paste was due to the epoxy group on the resin, which was crosslinked and cured with polybenzidine through ions. This solved the problem, in which the rigid molecular chains of polyaniline cannot be entangled, and have viscous flow. Furthermore, this realized the long-term dimension of the film structure, allowing the low-temperature high-conductivity silver paste to exhibit good film-forming performance and printing performance.

**Funding Statement:** The fund for this work was provided by the “Research on Key Technologies of Photosensitive Conductive Silver Paste Based on Domestic Circuit Protection Micro Chip Components” (Project No. BE2020008 and Supporting Author: Chen P).

**Conflicts of Interest:** The authors declare that there are no conflicts of interest related to the publication of this study.

## References

1. Mo, L., Guo, Z., Wang, Z., Yang, L. (2019). Nano-silver ink of high conductivity and low sintering temperature for paper electronics. *Nanoscale Research Letters*, 14(1), 197. DOI 10.1186/s11671-019-3011-1.
2. Ahammed, S. R., Susila, P. A. (2021). Direct writing of electronic circuits using functionalised multi-walled carbon nanotubes and polyvinyl alcohol conductive ink. *Advances in Materials and Processing Technologies*, 11, 1–14. DOI 10.1080/2374068X.2021.1913325.
3. Hou, C. M., Kou, Y. P., Cao, C. J. (2019). Preparation of conductive silver paste based on ethyl cellulose and properties of electronic paper. *Functional Materials*, 50(11), 11014–11018.
4. Camargo, J. R., Silva, T. A., Rivas, G. A., Janegitz, B. C. (2022). Novel eco-friendly water-based conductive ink for the preparation of disposable screen-printed electrodes for sensing and biosensing applications. *Electrochimica Acta*, 409, 139968. DOI 10.1016/j.electacta.2022.139968.
5. Zhuo, L., Liu, W., Zhao, Z., Yin, E., Li, C. et al. (2020). Cost-effective silver nano-ink for inkjet printing in application of flexible electronic devices. *Chemical Physics Letters*, 757, 137904. DOI 10.1016/j.cplett.2020.137904.
6. Ana, E. F. O., Arnaldo, C. P., Mayra, A. C. R., Lucas, F. F. (2022). Synthesis of a silver nanoparticle ink for fabrication of reference electrodes. *Talanta Open*, 5, 100085. DOI 10.1016/j.talo.2022.100085.
7. Lv, M., Zhao, R. H. (2021). Effect of the introduction and combination of silver nanoparticles with different morphologies on the electrical properties of conductive silver plasma. *Contemporary Chemical Research*, 12, 34–35.
8. Chung, Y., Byondi, F. K. (2021). 3D printed long-range cavity structure UHF RFID Tag antenna with painting conductive ink on convex surface. *Sensors*, 21(4), 1408. DOI 10.3390/s21041408.
9. Song, C. W., Yuan, S., You, L., Zhao, L., Pan, Y. Y. et al. (2020). Review of factors affecting the conductivity of low temperature cured conductive silver paste. *Marine Power Technology*, 40(12), 41–45.

10. Tao, R., Ning, H., Chen, J., Zou, J., Fang, Z. et al. (2018). Inkjet printed electrodes in thin film transistors. *IEEE Journal of the Electron Devices Society*, 6, 774–790. DOI 10.1109/JEDS.6245494.
11. Ning, T., Luo, Y., Liu, P., Lu, A. (2022). A novel Ag nanoparticles purification method and the conductive ink based on the purified Ag nanoparticles for printed electronics. *Journal of Nanoparticle Research*, 24, 15. DOI 10.1007/s11051-022-05401-x.
12. Du, Y. G., Yu, C. J., Wang, Z. (2016). Screen printability and rheology of conductive silver paste. *Precious Metals*, 37(2), 82–90.
13. Liu, C. (2016). *Effects of different solvents and resin molecular weights on the properties of low temperature cured conductive silver paste*. Shenzhen University, China.
14. Chen, Y., Zhan, H., Guo, J. (2021). Study on comprehensive properties of low temperature curing conductive silver paste based on bonding phase composition. *China Adhesive*, 30(10), 20–24.
15. Duić, L., Grigić, S. (2001). The effect of polyaniline morphology on hydroquinone/quinone redox reaction. *Electrochimica Acta*, 46(18), 2795–2803. DOI 10.1016/S0013-4686(01)00491-1.
16. Maeikien, R., Niaura, G., Malinauskas, A. (2021). Poly(N-methylaniline) vs. polyaniline: An extended pH range of polaron stability as revealed by Raman spectroelectrochemistry. *Spectrochimica Acta Part A: Molecular and Biomolecular Spectroscopy*, 262, 120140. DOI 10.1016/j.saa.2021.120140.
17. Mohamed, H. G., Aboud, A. A., Abd El-Salam, H. M. (2021). Synthesis and characterization of chitosan/polyacrylamide hydrogel grafted poly(N-methylaniline) for methyl red removal. *International Journal of Biological Macromolecules*, 187, 240–250. DOI 10.1016/j.ijbiomac.2021.07.124.
18. Maeikien, R., Niaura, G., Malinauskas, A. (2007). Electrochemical and in situ Raman spectroscopic study on the stability of poly(N-methylaniline). *Journal of Solid State Electrochemistry*, 11(7), 923–928. DOI 10.1007/s10008-006-0240-x.
19. Regina, M., Gediminas, N., Albertas, M. (2022). Raman spectroelectrochemical study of poly(N-methylaniline) at UV, blue, red, and NIR laser line excitations in solutions of different pH. *Spectrochimica Acta Part A: Molecular and Biomolecular Spectroscopy*, 274, 121109. DOI 10.1016/j.saa.2022.121109.
20. Abthagir, P. S., Saraswathi, R., Sivakolunthu, S. (2004). Aging and thermal degradation of poly(N-methylaniline). *Thermochimica Acta*, 411, 109–123. DOI 10.1016/j.tca.2003.08.010.
21. Mudiyansele, K., Trenary, M. (2009). Adsorption and thermal decomposition of N-methylaniline on Pt(1 1 1). *Surface Science*, 603, 3215–3221. DOI 10.1016/j.susc.2009.09.005.
22. Thiago, M. P., Lucas, G. S. C., Daniel, S. C., Sérgio, A. S. M. (2022). Homemade silver/Silver chloride ink with low curing temperature for screen-printed electrodes. *Journal of Electroanalytical Chemistry*, 915, 116316. DOI 10.1016/j.jelechem.2022.116316.
23. Shin, D. Y., Lee, Y. S., Kim, C. H. (2009). Performance characterization of screen printed radio frequency identification antennas with silver nanopaste. *Thin Solid Films*, 517, 6112–6118. DOI 10.1016/j.tsf.2009.05.019.
24. Wu, K., Hong, J., Qi, X., Ye, H., Li, Z. et al. (2022). Screen printing of silver nanoparticles on the source/drain electrodes of organic thin-film transistors. *Organic Electronics*, 106, 106524. DOI 10.1016/j.orgel.2022.106524.
25. Li, Y. S., Lu, Y. C., Chou, K. S., Liu, F. J. (2010). Synthesis and characterization of silver-copper colloidal ink and its performance against electrical migration. *Materials Research Bulletin*, 45, 1837–1843. DOI 10.1016/j.materresbull.2010.09.013.
26. Saeedeh, G. A., Saeedeh, M. B., Ali, M. B., Farhad, S. (2021). Effect of formulation and process on morphology and electrical conductivity of Ag-graphene hybrid inks. *Synthetic Metals*, 281, 116913. DOI 10.1016/j.synthmet.2021.116913.
27. James, R. D., Carrie, B., Alexander, C., Christopher, G., Berrigan, J. D. et al. (2020). Conductivity and radio frequency performance data for silver nanoparticle inks deposited via aerosol jet deposition and processed under varying conditions. *Data in Brief*, 33, 106331. DOI 10.1016/j.dib.2020.106331.
28. Salim, M. A., Hamidi, R., Saad, A. M. (2019). Overview of surface roughness effect on silver nanoparticle filled epoxy composites. *Encyclopedia of Materials: Composites*, 1, 628–670.

29. Chen, Y., Li, Q., Li, C., Dai, Z. F., Yan, H. et al. (2020). Regulation of multidimensional silver nanostructures for high-performance composite conductive adhesives. *Composites Part A*, 137, 106025. DOI 10.1016/j.compositesa.2020.106025.
30. Cao, G., Cui, H. H., Wang, L. L., Wang, T., Tian, Y. Q. (2020). Highly conductive and highly dispersed polythiophene nanoparticles for fabricating high-performance conductive adhesives. *ACS Applied Electronic Materials*, 2, 2750–2759. DOI 10.1021/acsaelm.0c00457.
31. Chen, S., Liu, K., Luo, Y., Jia, D., Gao, H. et al. (2013). In situ preparation and sintering of silver nanoparticles for low-cost and highly reliable conductive adhesive. *International Journal of Adhesion & Adhesives*, 45, 138–143. DOI 10.1016/j.ijadhadh.2013.04.004.